# Assessing the Global-Local Generalized Finite Element Method Techniques Using a Heterogeneous Bar

Thesis

Presented in Partial Fulfillment of the Requirements for the Degree of Bachelor's with Honors Research Distinction in the Undergraduate School of the Ohio State University

By
TJ Miller

The Ohio State University
2020

Thesis Committee:
Dr. Jack McNamara, Advisor
Dr. Patrick O'Hara
Troy Shilt

# Abstract

This thesis examines the generalized finite element method (GFEM) applied to a heterogeneous bar using global-local techniques to explore limitations and benefits of GFEM and global-local techniques. Overall structural behaviour is captured in a global problem, while local problems are used to capture fine-scale heterogeneities to capture local structural responses on coarser global meshes. GFEM uses local solutions as enrichments to allow coarse meshes to capture fine-scale behaviors. These techniques are applied to a model heterogeneous bar to explore accuracy and efficiency. The results are then further extended to investigate the how the displacement solutions change when various techniques are used to improve local solutions or conditioning of the GFEM matrices.

# Acknowledgments

The author of this thesis would like to thank the Ohio State University for the support in this project Furthermore, the support and guidance of Dr. Jack McNamara, Dr. Patrick O'Hara, and Troy Shilt for making this possible.

# Contents

# List of Figures

# 1 Introduction

The finite element method (FEM) is a numerical approach that seeks to approximate a solution by discretization of the problem domain into smaller "elements" (similar to numerical integration discretization) which then approximate part of a solution over each element using piece-wise continuous polynomials called shape functions. An extension of this method seeks to address the limitations of FEM, such as it's inability to approximate discontinuities on non-conforming meshes, or meshes that do not have nodes placed at every material interface, called the generalized FEM (GFEM). GFEM uses an added enriched trial space along with the FEM trial space to more accurately approximate localized features in a solution without the need for fine-scale meshes. This is done through the use of enrichment functions, derived from *a priori* knowledge of the solution, that approximate the behaviour of localized features. There exists much literature on GFEM, its benefits, applications to engineering problems and methods to improve its approximations [1-7]. One such method, which will be utilized in this thesis, is the global-local method.

Another method that will be utilized is SGFEM or stabilized GFEM [4]. SGFEM that seeks to address some of the limitations of GFEM, such as the inherent linear dependency of the stiffness matrix when all nodes of a mesh are enriched by GFEM functions. Normally, GFEM stiffness matrices need a specialized solution algorithm to solve since they are nearly singular (more details on this algorithm are presented in the Appendix), but global-local approximations use enrichment functions derived using FEM over a localized region of a problem domain to only enrich nodes within a subset of the local domain to retain the stiffness matrix linear dependence. Global-local approximations also remove the difficulty of deriving an enrichment function based on *a priori* knowledge since it is derived using FEM. This is useful for problems with complex geometries where analytically deriving an enrichment function is an involved process. On the other hand, SGFEM also addresses the problem of GFEM matrices being inherently linear dependent by reducing the condition number of the GFEM matrix by modifying the enrichment function. More details on SGFEM will be discussed in later sections.

While there is a wide variety of literature that explores the benefits and applications of GFEM and various methods associated with it, there is little

literature exploring its limitations and how to further improve approximations obtained with it. This thesis seeks to address the convergence and accuracy of GFEM using global-local approximation methods and SGFEM when compared to FEM on the same meshes. Several improvements to GFEM and global-local approximations such as: iterating the global-local solution, applying SGFEM in blending elements, and solving the initial global problem with homogeneous material and introducing the material interfaces later, are explored to address their ability to improve convergence and accuracy of the solution.

This thesis is organized as follows. Section 2 provides an outline of the various references used to research the GFEM process, global-local approximation method process, and the strategies used to improve global-local approximations and give insight into each methods benefits and why they are used. Section 3 gives a detailed analysis of the methods used to solve the model problem in this report. Section 3 presents the numerical results of each solution method used and provides displacement and convergence plots to graphically present results. Section 4 discusses the implications of the results and compares and contrasts each method, Section 5 provides a summary of the findings and concluding remarks. The problem explored in this report is detailed below and contains many material interfaces.

## 1.1 Problem Statement

The boundary value problem explored is the 1D heterogeneous bar with no externally applied forcing function, i.e., there is no distributed traction or body force applied to the bar. The governing differential equation for the bar is shown in Equation 1 below. All variables are assumed to be unit-less for simplicity.

$$-\frac{d}{dx}(E(x)A)\frac{du}{dx} = 0 \quad 0 \leq x \leq L \tag{1}$$

Where $E(x)$ is Young's Modulus of Elasticity as a function of $x$, $A$ is the cross sectional area of the bar, $u$ is the displacement function of the bar,

and $L$ is the length of the bar. For the current problem, $A = 1$ and $L = 1$. Equation 1 is subjected to the following boundary conditions presented as Equation 2 below.

$$\begin{cases} u(0) & = 0 \\ E(L)A\frac{du}{dx}(L) & = P \end{cases} \tag{2}$$

Where $P$ is a prescribed force applied to the bar. For the problem being studied in this report, $P = 10$. The Young's Modulus $E(x)$ is given as Equation 3 below.

$$E(x) = \begin{cases} E_H & 0 \leq x \leq \frac{3L}{8} \\ e(x) & \frac{3L}{8} < x < \frac{5L}{8} \\ E_H & \frac{5L}{8} \leq x \leq L \end{cases} \tag{3}$$

Where $E_H$ is the homogenized Young's modulus equal to 1.9512 and $e(x)$ is the periodic heterogeneous material. $e(x)$ is given by Equation 4 below.

$$e(x) = \begin{cases} E_1 & x \in \textit{ white phase} \\ E_2 & x \in \textit{ black phase} \end{cases} \tag{4}$$

Where $E_1$ is Young's modulus in the white phase equal to 1 and $E_2$ is Young's modulus in the black phase equal to 40. The length of each phase is equal to $\frac{L}{128}$. This model problem is illustrated in Figure 1

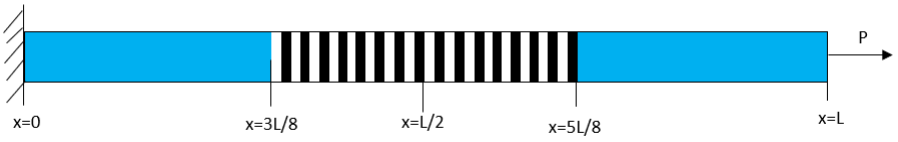


Figure 1: Model Bar with Heterogeneous Material

Figure 1 above shows the respective white and black phases of Young's modulus represented by Equation 4 and the homogenized regions represented by the solid blue sections of the bar. From Figure 1 above, the homogenized

material sections and heterogeneous material section occur in the domains outlined in Equation 3. The boundary conditions defined in Equation 2 are represented in Figure 1 by the clamp fixing the bar in space at $x = 0$ and the applied force $P$ at $x = L$. The exact solution of this problem is given as Equation 5 below.

$$u(x) = \begin{cases} \frac{P}{E_H}x & 0 \leq x \leq \frac{3L}{8} \\ \frac{P}{E_H}x + P\int_{\frac{3L}{8}}^{x} \frac{1}{e(x)}dx & \frac{3L}{8} < x < \frac{5L}{8} \\ \frac{P}{E_H}x + P\frac{L}{8}\left(\frac{1}{E_1} + \frac{1}{E_2}\right) + \frac{P}{E_H}\left(x - \frac{5L}{8}\right) & \frac{5L}{8} \leq x \leq L \end{cases} \tag{5}$$

# 2 Literature Review

This literature review studies the basics of the GFEM, its relation to the FEM, and the benefits this method provides when solving problems. This literature review also studies the global-local solution approach using GFEM and various methods to improve the global-local solution process to provide a better GFEM approximate solution.

## 2.1 Generalized Finite Element Method

The GFEM is an extension of the FEM in which the finite element space is modified using enrichment functions derived from *a priori* knowledge about the solution of a problem. In other words, this can be interpreted as the FEM with an enriched trial space obtained by hierarchically augmenting a FEM approximation space with a enrichment space [1]. GFEM shape functions, basis functions of a GFEM enrichment space, are calculated as the product of a FEM shape function and an enrichment function. Thus, the process of solving a GFEM matrix is identical to that of a FEM matrix and boundary conditions are applied in the same way if the enrichment functions are zero at the nodes (this is done through shifting the enrichment's) [1]. Enrichment functions are selected to better approximate local features of a solution such as discontinuities, singularities, material interfaces, etc. using knowledge of the solution beforehand. Thus, these features are captured by the enrichment's instead of the FEM shape functions [1].

If the FEM shape functions are chosen to be Lagrangian shape functions, then by the definition of a GFEM shape function, any enrichment function can be reproduced in an element within the GFEM mesh [1,2]. This is due to Lagrangian shape functions creating a partition of unity over each element. However, this also means that GFEM stiffness matrices are inherently linearly dependent since the enrichment function is reproduced in each enriched element when polynomial enrichment's are used [1]. The definition of the GFEM shape function also shows that the approximation space that the GFEM solution will exist in is on the order of *p+1*, where p is the order of the GFEM enrichment functions since this report is concerned with using only linear FEM shape functions to solve the given problem. Thus, solving GFEM stiffness matrices where every node has been enriched requires a solution algorithm and is computationally inefficient [2]. To circumvent this issue, FE meshes can be enriched locally to capture specialized features of a solution by only enriching a local subset of nodes in a mesh and retain linear independence [2].

Although local enrichment corrects the inherent linear dependence of a GFEM stiffness matrix, it presents another problem in handling blending elements [1,2]. Blending elements are elements in the FE mesh that only have some nodes enriched and not all. Consequently, elements who have every node enriched by an enrichment function are called reproducing elements and those with no enriched nodes are called standard FEM elements [2]. Blending elements pose a problem in solving GFEM matrices because they introduce parasitic terms into the element stiffness matrix since the enrichment function cannot be exactly reproduced since the partition of unity is lost in the GFEM shape functions when only part of an element is enriched. Though blending elements can cause errors to arise in the solution, they do not pose a problem when the applied enrichment's are constant or zero in the blending elements [2]. Thus for the problem studied in this report, blending elements are of concern since the enrichment's used will not be constant or zero in the blending elements.

GFEM is relevant to the problem studied in this report since it includes multiple material interfaces which pose weak discontinuities in the exact solution of the problem. Therefore, an appropriate enrichment function can be selected to approximate the solution in the regions where material interfaces occur and use a coarser mesh to obtain a solution. This type of problem

would require a fine FEM mesh in order to reproduce the exact solution since FEM with Lagrangian polynomials would need to place nodes at each material interface to accurately approximate their effect on the solution. Thus, GFEM allows the potential to study selection of enrichment functions where convergence can be achieved before the required FEM condition is reached for convergence and study its ability to approximate localized features when nodes are not placed on points of discontinuity. The exact formulation of the GFEM process will be outlined later in this report.

## 2.2 Stable Generalized Finite Element Method

The stable generalized finite element method (SGFEM) is an extension of GFEM that sought to address the poor numerical conditioning of large GFEM matrices [4]. This method modifies the enrichment function used by subtracting a linear approximation, that is approximating the enrichment as a straight line, of the enrichment over an element or cloud from the enrichment function itself. By doing this, the results of [4] show that a significant reduction in the matrices conditioning number occur and the growth rate of the condition number is much slower compared to using GFEM for the same problem. SGFEM has also been shown to reduce errors and improve the convergence rate of the numerical solution compared to GFEM. This is relavent to the problem explored in this report since the GFEM mesh is locally enriched leading, that the enrichment functions are only applied in certain elements, to the formation of blending elements which can potentially cause errors in the solution since the partition of unity is lost in these elements. Using SGFEM can potentially stabilize these elements and reduce errors in them. The exact formulation for SGFEM will be discussed in a later section.

## 2.3 Material Interfaces

Material interfaces are points in a problem domain where a material change occurs, that is the material properties of the problem change across this point [2,3]. This introduces a discontinuity into the problem solution because the change in material properties across these points causes the derivative of the problem solution to have two slope values at the same point. This is labeled as a weak discontinuity since the discontinuity only exists in the first deriva-

tive of the solution while the solution itself is continuous [1,2,3]. In standard FEM, these material interfaces are handled by placing nodes at the points where they occur, which complicates the meshing step for problems with complex geometries. Using GFEM to solve these type of problems removes this constraint and simplifies the meshing step since each element in the mesh doesn't have to be homogeneous with appropriate selection of an enrichment function [3]. [3] explores using the level set function with the signed distance function to create an enrichment function with a weak discontinuity to approximate material interfaces with non-conforming elements. It was shown that using GFEM with these types of enrichment's can achieve optimal convergence rates when compared to FEM using conforming elements at the material interfaces.

The methods used in [1,2,3] to handle material interfaces are relevant to the problem at hand since the geometry introduces many material interfaces that must be appropriately approximated. The results of [3] motivate using enrichment's with weak discontinuities to solve problems with material interfaces to achieve optimal convergence rates. This will also simplify the meshing step and geometrical data pre-processing.

## 2.4 Global-Local Approximation

Global-local approximations are similar to the concept of GFEM in which these methods utilize a fine-scale local approximation over a local domain to more accurately approximate specialized features in a problem solution and apply it to the coarser global scale problem. This method was originally used in pure FEM problems by solving an initial coarse global problem and then solving a fine scale local problem over a local domain using values obtained from the initial global problem as boundary conditions for the local problem, then modifying the force vector of the global problem with the local solution to more accurately represent localized features [5]. In other words, the local solution is used to create a "supplementary force vector" which is added to the initial global problem force vector to account for localized features that the initial global problem cannot capture [5]. Although this method was initially developed for FEM, its extension to GFEM is straight-forward and follows a similar process outlined in [6].

The application of global-local methods to GFEM follows the same procedure as FEM. First a coarse global-problem is solved using FEM, then a local problem is solved over a localized domain of interest using values obtained from the initial global problem as boundary conditions. Then, the local solution is used as an *enrichment function* and applied to the same global mesh before solving the enriched global problem [6]. This method has been shown to reduce computational costs compared to FEM solutions of identical accuracy [6]. It also allows for the derivation of an enrichment function without *a priori* knowledge of a solution since the enrichment function is formulated using FEM over a local domain [6]. This is beneficial since for more complicated geometries and problems, deriving a appropriate enrichment function can be a daunting task.

Though global-local approximation lower computation cost without the need to sacrifice accuracy, the accuracy of the resulting enriched global problem is directly dependent on the accuracy of the local problem and thus the initial global problem. To rectify this, it has been suggested to iterate the global-local process to update boundary conditions for the local problem using values obtained from the enriched global problem to improve the accuracy of the local problem and thus the enriched global problem [5,6]. This method will be explored in this report to analyze its effectiveness when applied to the current problem along with a pure global-local approach.

# 3 Methodology

The methods used to solve the model problem include the GFEM and its application in global-local approximation methods, as well as, various methods to improve the global-local approximation solution. This section will be divided into three parts to outline the formulation of each method used. These sections will give an overview of the formulation using the GFEM, an outline of global-local approximation methods applied to the GFEM, and an outline of the various methods used to improve the global-local solution.

## 3.1 Overview of the GFEM

The generalized finite element method(GFEM) is an extension of the FEM and a specialized case of the partition of unity methods. A brief overview of its formulation and application will be presented here. A more detailed look at the GFEM can be found in the works [1-2].

The GFEM uses Lagrangian finite element shape functions $N_\alpha$, where $\alpha$ exists within the set of nodes associated with the shape functions with $n$ nodes over the problem domain, as the partition of unity since they satisfy the partition of unity requirement given by Equation 6 below.

$$\sum_{e \in I_h} N_\alpha(x) = 1 \tag{6}$$

Where $I_h = \{1, \ldots, n\}$ is the set of all $n$ nodes in the GFEM mesh and $N_\alpha$ are the set of Lagrangian shape functions in the GFEM mesh. The GFEM is built on the idea that the partition of unity can be enriched, that is the standard FE approximation space can be augmented with an enrichment space derived from *a priori* knowledge about the solution of a problem. The basis functions of a GFEM enrichment space are then given by the product of a Lagrangian FE shape function and an enrichment function and denoted as a GFEM shape function. Equation 7 below shows how these shape functions are calculated.

$$\phi(x) = N_\alpha(x) E_{\alpha j}(x), \quad \alpha \in I_h^e \subset I_h \quad j \in \{1, \ldots, m_\alpha\} \tag{7}$$

Where $\phi(x)$ is the GFEM shape function, $E_{\alpha j}$ is the enrichment function, $I_h^e$ is the set of enriched $m_\alpha$ nodes and $j$ is the set of enrichment functions associated with $\alpha$ nodes. The set of nodes $I_h$ and $I_h^e$ can differ from one another. This means that if $\alpha$ is in $I_h$, but not $I_h^e$ then the nodes only contain FEM shape functions. The GFEM trial space, $S_{GFEM}$, is built by hierarchically augmenting the FEM trial space, $S_{FEM}$, with the enrichment space, $S_{ENR}$, this is given as Equation 8 below.

$$S_{GFEM} = S_{FEM} + S_{ENR} \tag{8}$$

The FEM and enrichment trial spaces are defined by Equations 9 and 10

respectively below.

$$S_{FEM} = \sum_{\alpha \in I_h} \hat{u}_\alpha N_\alpha(x) \quad \hat{u}_\alpha \in \Re \tag{9}$$

$$S_{ENR} = \sum_{\alpha \in I_h^e} \sum_{j=1}^{m_\alpha} \tilde{u}_{\alpha j} \phi_{\alpha j}(x) \quad \tilde{u}_{\alpha j} \in \Re \tag{10}$$

Where $\hat{u}_\alpha$ are the standard FEM degrees of freedom associated with node $\alpha$ and $\tilde{u}_{\alpha j}$ are the enriched degrees of freedom associated with node $\alpha$ and enrichment $j$. With this, a GFEM approximation $u^h(x)$ of a scalar field $u(x)$ belonging to the space $S_{GFEM}$ is given by Equation 11.

$$u^h(x) = \sum_{\alpha \in I_h} \hat{u}_\alpha N_\alpha(x) + \sum_{\alpha \in I_h^e} \sum_{j=1}^{m_\alpha} \tilde{u}_{\alpha j} \phi_{\alpha j}(x) \tag{11}$$

Where the first part of Equation 11 is the standard FEM approximation and the second part is the enriched GFEM approximation. This is reflected in Equation 8 since the GFEM approximation space is sum of the enriched and FEM approximation spaces. The formulation of the force vector and the stiffness matrix for a GFEM approximation is identical to that of the procedure for FEM. The application of boundary conditions in GFEM is also identical to the process in FEM as long as the enrichment functions are zero at the nodes. To achieve this, the enrichment functions used are modified to be *shifted* at the nodes as given by Equation 12 below.

$$u^h(x) = \sum_{\alpha \in I_h} \hat{u}_\alpha N_\alpha(x) + \sum_{\alpha \in I_h^e} N_\alpha(x) \sum_{j=1}^{m_\alpha} \tilde{u}_{\alpha j} (E_{\alpha j}(x) - E_{\alpha j}(x_\alpha)) \tag{12}$$

By shifting the enrichment's at the nodes, the enrichment function will be zero at the nodes which means no special treatment of boundary conditions is necessary and the imposition of boundary conditions is straight forward like in FEM.

### 3.1.1 SGFEM Formulation

To apply SGFEM to a given problem, the enrichment function are slightly modified. The form SGFEM enrichment functions take is shown in Equation 13 below.

$$\tilde{E}_{\alpha j}(x) = E_{\alpha j}(x) - I_{\omega\alpha}(E(x)) \tag{13}$$

Where $I_{\omega\alpha}(E_{\alpha}j(x))$ is a piece-wise linear finite element interpolant of the enrichment function. All other steps in the GFEM process remains the same in SGFEM. SGFEM only modifies the enrichment used to stabilize the resulting global matrix.

### 3.1.2 Shape Functions

For the problem explored here, only linear FEM shape functions are used to approximate the solution of the problem. This is due to the problem being a hetergeneous material problem with no singularities or sharp gradients in the displacement solution. This means that the problem solution will be a series of piece-wise linear functions and thus higher order FEM shape functions are not needed to capture the general behavior of the solution. GFEM and global-local approximations are used to capture the localized features caused by the heterogeneous materials. The linear FEM shape function over an element is given by Equation 14.

$$N_{\alpha}(x) = \begin{cases} \frac{x - x_i - 1}{x_i - x_{i-1}} \\ \frac{x_{i+1} - x}{x_i - x_{i-1}} \end{cases} \tag{14}$$

Where $i$ is the nodal index of the point associated with a node in the mesh. Since FEM and GFEM integration transforms shape functions to a local coordinate system associated with each individual element, it is more useful to transform Equation 14 into the local coordinate system via iso-parametric mapping of the global coordinate. The formula used to interpolate the $x$ coordinate within an element is given by Equation 15.

$$x(\epsilon) = \frac{1 - \xi}{2} x_i + \frac{1 + \xi}{2} x_{i+1} \tag{15}$$

where $\xi$ is the local elemental coordinate and varies from -1 to 1 in an element. Plugging this into Equation 14 yields Equation 16 below.

$$N_\alpha(\xi) = \begin{cases} \frac{1-\xi}{2} \\ \frac{1+\xi}{2} \end{cases} \tag{16}$$

Notice that the shape functions in Equation 16 are interpolated the same way the x-coordinate in Equation 15 is, thus showing that iso-parametric mapping was used. The shape functions shown in Equation 16 are used for all FEM and GFEM approximations in this report.

## 3.2 Stiffness Matrix and Force Vector Formulation

The formulation of an elemental stiffness matrix and force vector for a GFEM element is identical to the process required to calculate these two components in FEM. For a 1D problem, calculation of the stiffness matrix requires the differentiation and integration of the piece-wise shape functions over each element. The formula used to calculate each elemental stiffness matrix is given by Equation 17 below.

$$k_e = \int_{x_i}^{x_{1+1}} E(x)A(x)\frac{d\phi(x)}{dx}^T \frac{d\phi(x)}{dx} dx \tag{17}$$

Where $\phi(x)$ is the vector set of shape functions in an element. The equation above can be rewritten using the elemental local coordinate using Equations 15 and 16. The form Equation 17 takes when written in the elemental local coordinate is given by Equation 18 below.

$$k_e = \int_{-1}^{1} E(\xi)A(\xi)\frac{d\phi(\xi)}{dx}^T \frac{d\phi(\xi)}{dx}\frac{1}{J} d\xi \tag{18}$$

Where $J$ is the Jacobin which is equal to the derivative of the coordinate transformation given in Equation 15. It is typically easier to work in a local coordinate for FEM and GFEM formulations and thus the equation used to calculate the force vector will be given in terms of the local coordinate system. The force vector for a given element is calculated by Equation 19 below.

$$f_e = \int_{-1}^{1} b(\xi)\phi(\xi)^T J d\xi + f_n \tag{19}$$

Where $b(\xi)$ is the body force function and $f_n$ is the vector of point loads acting on the nodes. Equation 18 and 19 together represent a static equilibrium system of equations in the $e$th element. The solution of the entire bar will come from the elemental stiffness matrices and force vectors assembled into one global matrix and vector. Each elemental stiffness matrix or force vector is assembled into its global counterpart simply by adding together elements of the matrices or vectors that are calculated from shared nodes in the GFEM mesh. The solution of which will yield the displacement of the degree of freedoms at each node, which can then be applied to Equation 12 to obtain the general solution of the bar. Equation 20 below shows the form the global system of equations take when solving for the displacement solution.

$$KU = F \tag{20}$$

Where $K$ is the global stiffness matrix, $F$ is the global force vector, and $U$ is the global displacement vector (vector that collects all the degrees of freedom in the GFEM mesh). Equation 20 can be solved with matrix solving algorithms, such as Gaussian elimination, to solve for $U$.

## 3.3 Global-Local Approximation Method

Global-local approximations allow a problem with specialized features that cannot be captured using a coarse mesh to be solved on coarser meshes by solving the problem on a *local domain*. Solving the problem on a local domain can capture these specialized features and reapplying the local solution on the global mesh can capture these localized features on a coarse mesh. The global-local approximation method for GFEM is slightly different then for a problem solved purely using FEM.

### 3.3.1 The Initial Global Problem

The initial global problem process is no different from applying FEM normally to a problem. This step only involves solving the given problem only

using FEM with appropriate shape functions to capture the solution as accurately as possible. The main purpose of this step is to provide boundary conditions to be used in the local problem to solve the problem on a local domain to capture localized features of interest. Thus, the accuracy of the initial global problem directly impacts the accuracy of the local problem and in turn the final enriched global problem. This is why it is necessary for the initial global problem to be as accurate as possible so this method will show optimal convergence. The initial global problem solution will be labeled as $u_G^0(x)$. The initial global problem follows the same steps for GFEM that were outlined previously, except the problem will only be solved with FEM elements and no enrichment functions.

### 3.3.2 Local Problem

The local problem solution process is also identical to solving any process with FEM since this step will only use FEM to obtain its solution. This step, however, uses information obtained from the initial global problem to approximate the solution of a problem on a local domain. That is, this problem will only be solved on a subset of x-coordinates in the global domain to capture localized features in the problem. Thus, this problem will apply Dirichlet boundary conditions at the endpoints of the local domain obtained from the initial global problem at the same points. For the model problem studied in this report, the local domain will span $\Omega_L = \{x|\frac{L}{4} < x < \frac{3L}{4}\}$. Equation 21 below shows the boundary conditions that will be applied to the local problem.

$$\begin{cases} u_L(\frac{L}{4}) = u_G^0(\frac{L}{4}) \\ u_L(\frac{3L}{4}) = u_G^0(\frac{3L}{4}) \end{cases} \tag{21}$$

Where $u_L(x)$ is the local solution. As mentioned, only linear shape functions will be used to solve the local and initial global problem utilizing only FEM.

### 3.3.3 Enriched Global Problem

The enriched global problem uses the solution obtained from the local problem using FEM as an enrichment to apply GFEM on the same mesh as the

initial global problem. This is done so that the problem can be solved on a coarse mesh and still accurately capture localized features in the problem. This also has the advantage of mitigating the need for *a priori* information to analytically derive an enrichment function since the local problem will create the enrichment function using FEM. This problem is then solved using the GFEM process outline above. However, it must be noted that the accuracy of the solution obtained using this method is directly affected by the accuracy of the local solution since if the local solution does not effectively capture the localized features, the enriched global problem will not be able to either. For the enriched problem, nodes in the mesh in the range of $I_h^e = \left[\frac{3L}{8}, \frac{5L}{8}\right]$ will be enriched with the chosen enrichment function. It should be noted that by fixing the $I_h^e$ the number of nodes enriched as the number of elements increase also increases.This was selected as the set of nodes to enrich since it contains the heterogeneous material section which is the localized feature that is captured with the GFEM shape functions. It is also possible to extend the local problem to cover the entire problem domain and use a fine mesh to capture the exact behaviour of the problem solution and use that as an enrichment for the GFEM problem. This will be explored in the following sections to observe of the GFEM solution changes when all nodes are enriched with the exact solution of the problem. The solution of the enriched problem will be labeled $u_G^E(x)$.

## 3.4 Global-Local Approximation Method Improvements

There have been several methods in literature suggested to improve the approximations obtained by using global-local approximations methods. A few suggested [5,6] will be explored here. These methods will be used to solve the model problem presented in this report and compared to each other to determine each methods effectiveness.

### 3.4.1 Iteration

The first method tested was to iterate the global-local method to obtain a better solution by updating the boundary conditions used to formulate the local solution. This is done by solving the problem by the global-local method as normal and then using the enriched solution to obtain more accurate

boundary conditions for the local problem. That is, the updated boundary conditions are obtained by Equation 22 below.

$$\begin{cases} u_L(\frac{L}{4}) = u_G^E(\frac{L}{4}) \\ u_L(\frac{3L}{4}) = u_G^E(\frac{3L}{4}) \end{cases} \tag{22}$$

Then, these boundary conditions are used to resolve the local problem to obtain a more accurate local solution and this is reapplied to the enriched problem as a enrichment and resolved. This, in theory, should provide a more accurate solution since a more accurate enrichment is used to solve the problem. This iteration process can be repeated as much as possible until convergence occurs. However, [5] has suggested that not more than one iteration is necessary to obtain convergence for a given element size. This is because the solution obtained after one iteration does not tend to change with more iterations and thus the local solution will not improve, as well, as the enriched solution.

### 3.4.2 Homogenizing the Problem

Since the model problem is a heterogeneous material problem with the same material constant used before and after the local domain that includes the heterogeneous materials, the problem can be homogenized to directly obtain the correct boundary conditions for the local problem and thus reproduce the exact solution in the local domain. This is done by setting the material constant of the entire domain equal to $E_H$ and solving the initial global problem with this. The boundary conditions obtained from this solution will then match the exact solution at the end points of the local domain. The local problem and enriched problem are then solved as usual. This method was used to force the local problem to match the exact solution to study how the accuracy of the local solution affected the enriched problem.

### 3.4.3 Stabilizing the Blending Elements

This method applies SGFEM in the blending elements of the GFEM mesh to stabilize these elements and reduce errors in the solution. SGFEM is only applied in the blending elements while the formulations of all other elements

remains the same. Blending elements can cause problems in GFEM solutions since the partition of unity used to build shape functions and reproduce enrichment's within an element is lost in these elements. This can cause poor conditioning of the resulting global stiffness matrix and produce errors in the solution. SGFEM was used in these elements to improve the conditioning of the matrix and reduce errors in the solution. This method was used without iterating the solution or homogenizing the problem so that it could be compared to other methods. Although, it is possible to combine this method with those previously mentioned to further improve results.

## 3.5 Error Analysis

To verify and analyze the accuracy of the GFEM solution, the strain energy of the approximations were calculated and compared to the exact strain energy calculated from the exact solution according to the methods outlined in [7]. This was done for every element order used to solve the problem. The strain energy for the exact solution and the GFEM solutions were computed using Equations 23 and 24 below.

$$U = \frac{1}{2}\int_0^L EA\Big(\frac{du}{dx}\Big)^2 dx \tag{23}$$

$$U_G^E = \frac{1}{2}u_G^E F \tag{24}$$

where $U$ is the strain energy of the exact solution, $U_G^E$ is the strain energy of the GFEM solutions, $u$ is the exact solution, and $F$ is the force vector. The strain energy was then used to calculate the error in the energy norm with Equation 25 below.

$$e_r = \sqrt{\frac{U - U_G^E}{U}} \tag{25}$$

Where $e_r$ is the error in the energy norm. The errors were then used to construct log-log plots of the error in the energy norm versus the number of total degrees of freedom in the mesh. These plots were then used to compute the convergence rate of a given method and verify each methods effectiveness

in approximating the solution. The plots were then used to compare each method and FEM solutions to determine how well each method approximates the solution and how fast each method converges.

# 4 Results

This section presents the numerical results obtained from applying the GFEM and the global-local approximation methods to the model problem. The results presented will show the displacement plots created from the results of the GFEM with the global-local method and the various improvements to it applied as well. The plots will also show the initial global problem, the local solution and the exact solution for comparison purposes. This section will also present the convergence plots for each method to verify each methods effectiveness and the convergence rates. All displacement plots were created using eight global elements and 128 local elements to ensure that the local solution captures the behaviour of the heterogeneous material section. Figure 2 below shows the displacement solution obtained using the global-local approximation method and the GFEM to solve the model problem and only enriching the nodes contained in the set of nodes defined as $I_h^e = \left[\frac{3L}{8}, \frac{5L}{8}\right]$.

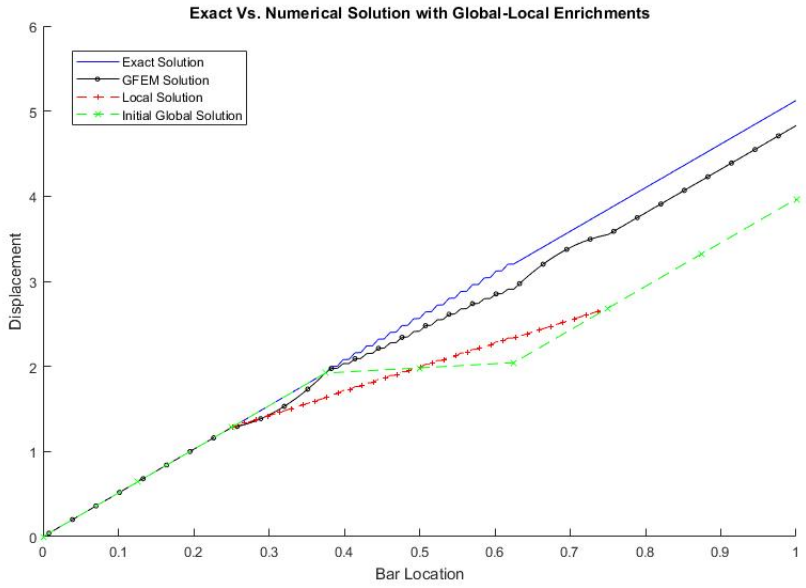


Figure 2: Displacement Solutions of the Model Problem Using Global-Local GFEM with First Iteration Local Solution

Figure 2 above shows the exact, local, initial global, and GFEM solutions as mentioned before. From the plot above, the local problem does not match the exact solution in the same domain which is reflected in the initial global solution since the this solution does not agree with the exact solution as well. The GFEM solution matched the exact solution up until $x$ equals 0.25 then the solution diverges. However, the GFEM solution still captures the general behaviour of the heterogeneous material section. It can also be observed that the slope of the GFEM solution after the heterogeneous material section matches that of the exact solution despite inconsistencies in the point values. The portions of the solution that contain the blending elements can also be observed in the GFEM solution by the "bubbles" that appear in the plot since the GFEM approximation in the blending elements is quadratic. Figure 3 below shows the displacement plots of the bar solved using the same methods that produced Figure 2, but homogenizing the initial global problem.

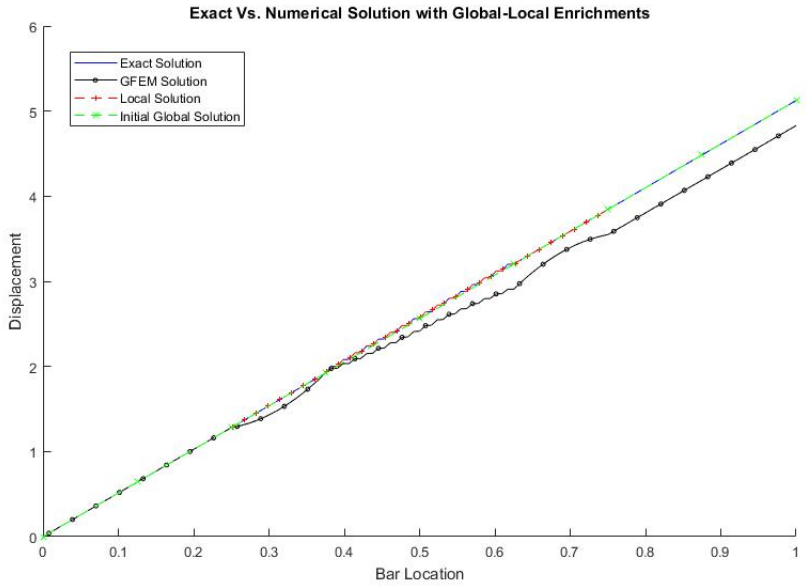


Figure 3: Displacement Solutions of the Model Problem Using Global-Local GFEM with Exact Local Solution

From Figure 3 above, it can be seen that the local solution matches that of the exact solution and that the initial global problem is a straight line of constant slope due to the homogenization of the problem. The GFEM solution, however, has not changed despite the improvement in the local solution. This trend persists in other methods used to solve the model problem which will be shown. Figure 4 below shows the displacement solutions obtained using the same methods used to produce Figures 2 and 3 above, but a constant enrichment equal to one was used to enrich nodes outside the set of nodes contained in $I_h^e$.

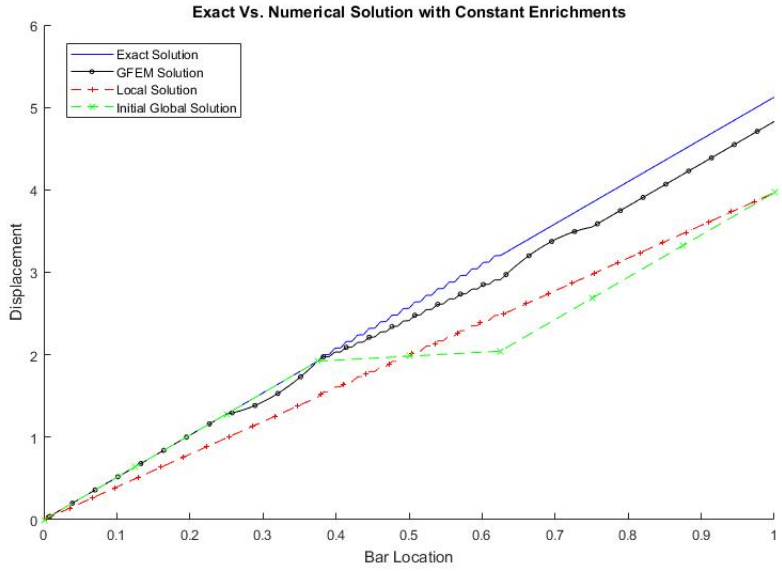


Figure 4: Displacement Solutions of the Model Problem Using Global-Local GFEM with First Iteration Local Solution and Constant Enrichments

From Figure 4 above, the results match those presented in Figure 2 with regards to the GFEM solution when using a local solution that does no agree with the exact solution. Figure 5 below shows the displacement solution using the same methods used to produce Figure 4, but with the initial global problem homogenized to produce a local solution that matches the exact solution like in Figure 3.

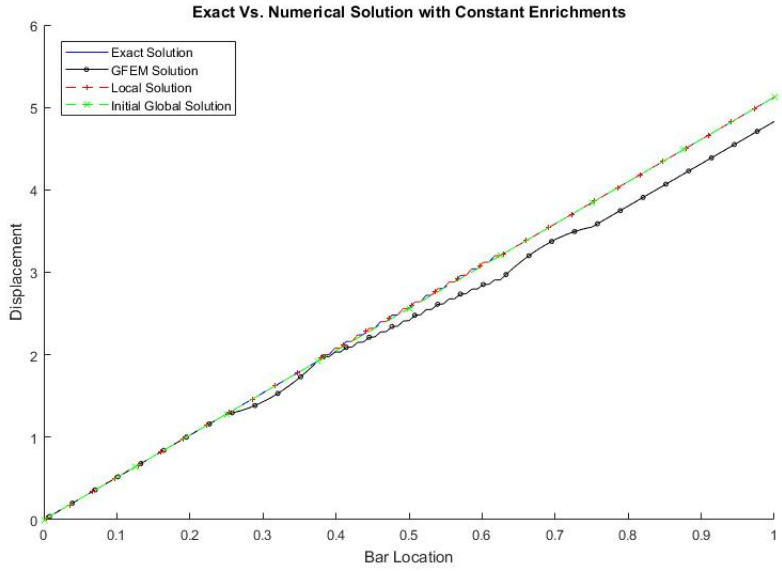


Figure 5: Displacement Solutions of the Model Problem Using Global-Local GFEM with Exact Local Solution and Constant Enrichments

From Figure 5 above, the results shown match those observed in each of the previous three figures. This demonstrates that using constant enrichments has no impact on the GFEM solution whether the local solution matched the exact solution or not. Figure 6 below shows the displacement solutions obtained using a local solution that extends the entire problem domain and enriching every node in the GFEM mesh.

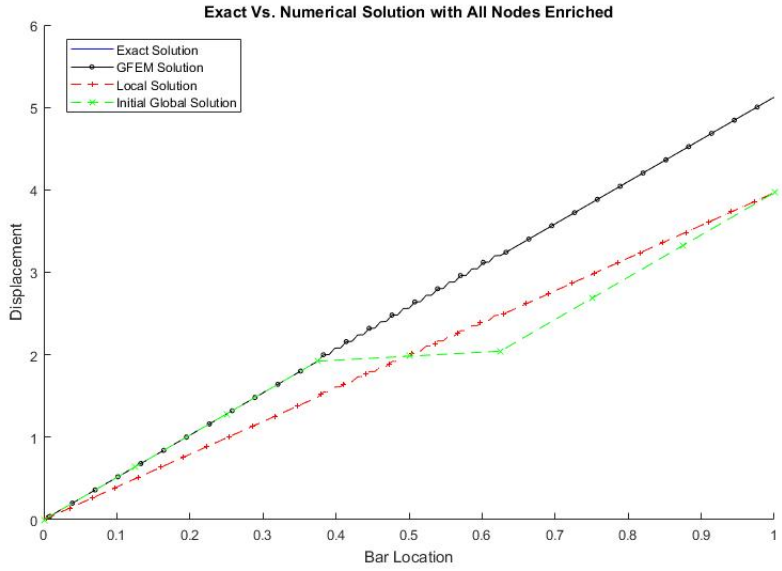


Figure 6: Displacement Solutions of the Model Problem Using Global-Local GFEM with First Iteration Local Solution and All Nodes Enriched

From Figure 6 above, the GFEM solution agrees with the exact solution with only eight elements used when all nodes were enriched with a local solution that extended the entire problem domain. The GFEM solution captures the behaviour of the exact solution without the local solution matching the exact solution. Figure 7 below shows the displacement solution obtained when using a local solution that matches the exact solution and enriching all nodes in the GFEM mesh.

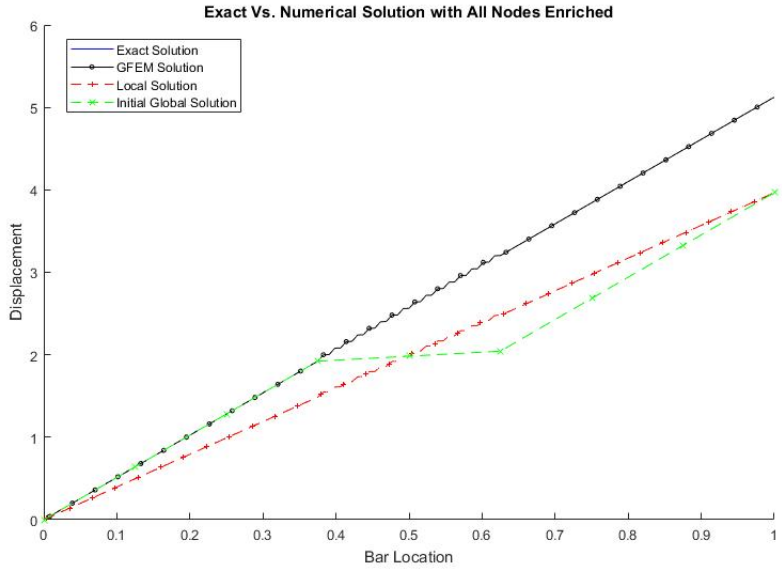


Figure 7: Displacement Solutions of the Model Problem Using Global-Local GFEM with Exact Local Solution and All Nodes Enriched

From Figure 7 above, the results presented match those presented within Figure 6. This demonstrates that the local solution need only capture the general behavior of the heterogeneous material section to obtain complete convergence in the GFEM solution. Figure 8 below shows the displacement solutions obtained when the model problem was solved using global-local methods to enrich the nodes contained in $I_h^e$ and applying SGFEM in the blending elements.

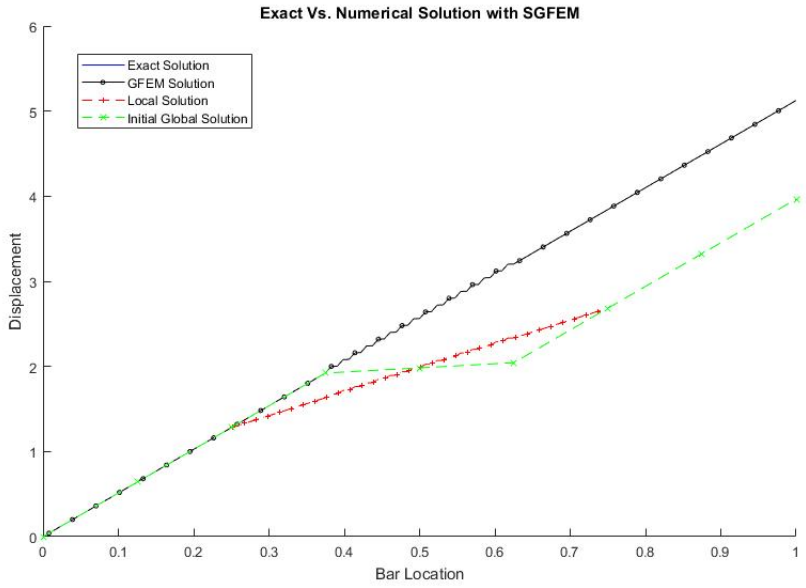


Figure 8: Displacement Solutions of the Model Problem Using Global-Local GFEM with First Iteration Local Solution and SGFEM in the Blending Elements

From Figure 8 above, the GFEM solutions reproduces the exact solution despite the local solution disagreeing with the exact solution, as was observed in Figure 6. Figure 9 below shows the displacement solutions obtained using the same method used to produce Figure 8, but with the local solution matching the exact solution.

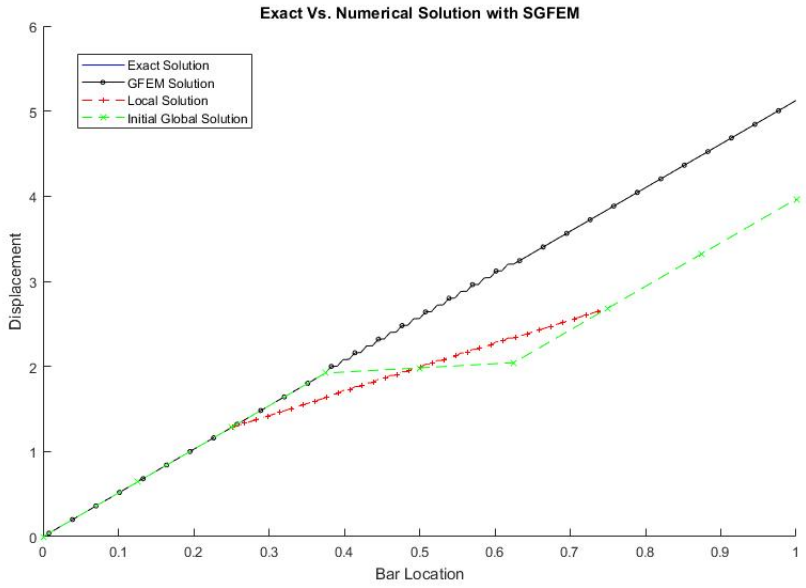


Figure 9: Displacement Solutions of the Model Problem Using Global-Local GFEM with Exact Local Solution and SGFEM in the Blending Elements

From Figure 9 above, as was observed in Figure 8, the GFEM solution is identical to the exact solution. This further demonstrates what was observed in Figures 6 and 7, that the local solution need only capture the general behaviour of the localized features to reproduce the exact solution once the the GFEM mesh is stabilized. Figure 10 shows the convergence plot of the global-local GFEM method compared to that of the FEM.

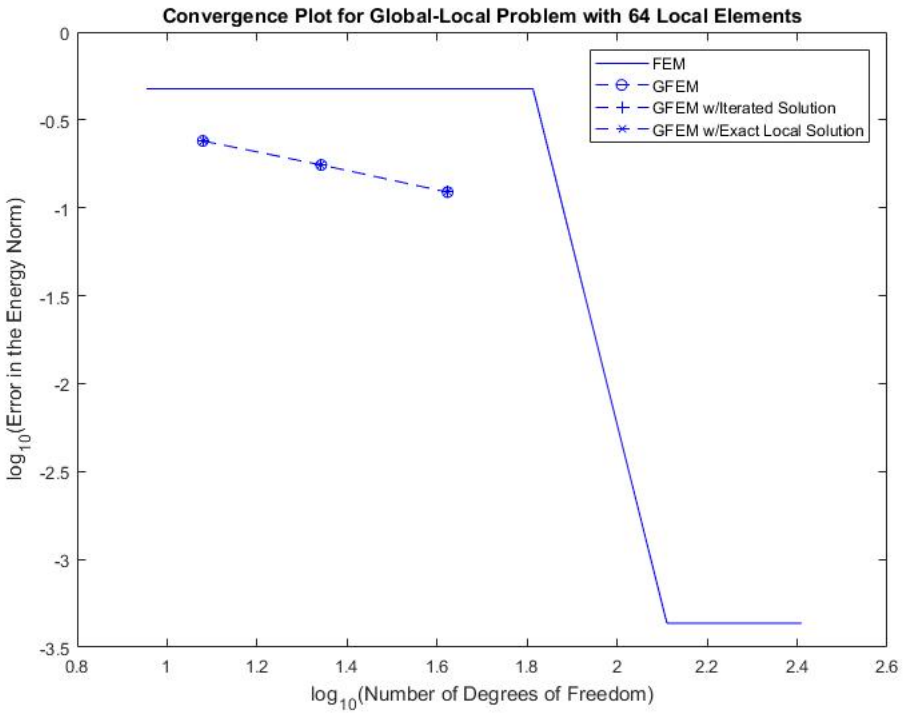


Figure 10: Convergence Plot with 64 Local Elements Used

Figure 10 above shows the error in the energy norm versus the number of degrees of freedom used on a log-log scale. All convergence plots are graphed on log-log scales to observe each methods convergence rate as was discussed in Section 3.5. From the figure above, the error in the FEM solutions strain energy remains constant until 128 elements are used, then there is an almost discontinuous jump in the error as the approximation in the strain energy significantly improves when 128 elements or more are used. This jump in the error is due to the FEM solution converging to the exact solution when 128 global elements are used. By using 128 elements, a node is placed at each material interface which allows the FEM solution to accurately capture the effect of the changing materials in the numerical solution. For the GFEM solutions, the error in the strain energy shows a linear convergence rate when equal to 0.53. This demonstrates that the local solution has captured the behavior of the heterogeneous material section when only 64 local elements are used to solve the problem. Figure 10 above also shows that the error in the

energy norm for the iterated global-local GFEM and the GFEM solution that uses the exact local solution all have the same values compared to the global-local GFEM with no improvements. Figure 11 below shows the convergence plot of the global-local GFEM when 128 local elements were used.

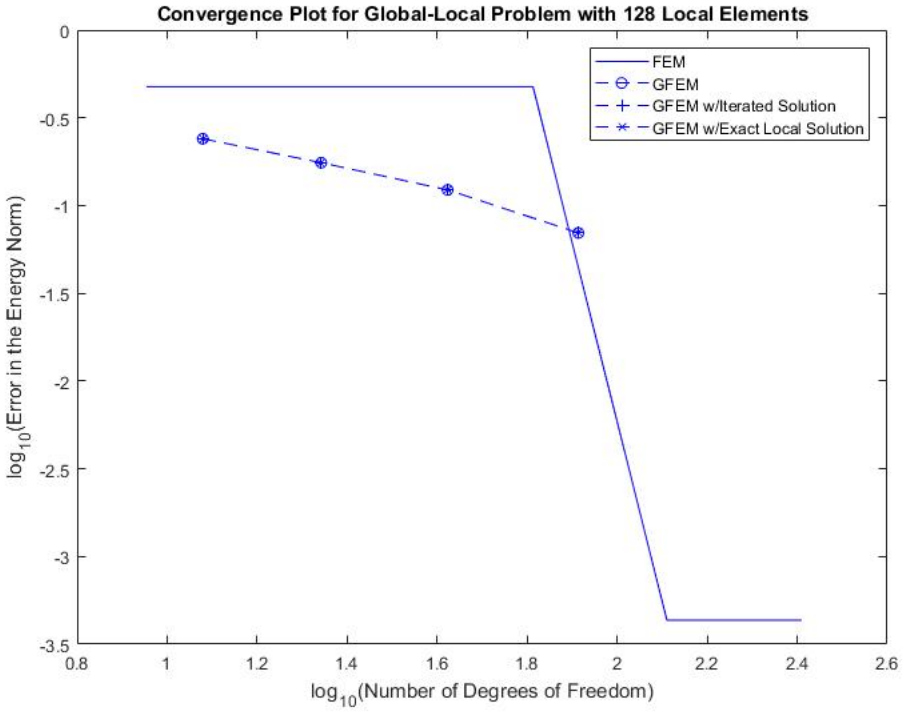


Figure 11: Convergence Plot with 128 Local Elements Used

Figure 11 above shows that the error in the energy norm from 12 to 42 degrees of freedom match the values presented in Figure 10. This further demonstrates that the local solution has captured the general behavior of the local problem and thus increasing the number of local elements does not improve the local problems approximation. The figure above also shows that the convergence rate is still linear and equal to 0.53 like before. As was shown in Figure 10, Figure 11 also shows that for each global-local improvement method used there was no change in the error in the energy norm and all values match. Figure 12 below shows the convergence plots for the FEM and GFEM with all improvement methods applied and using 256 elements in the local problem.

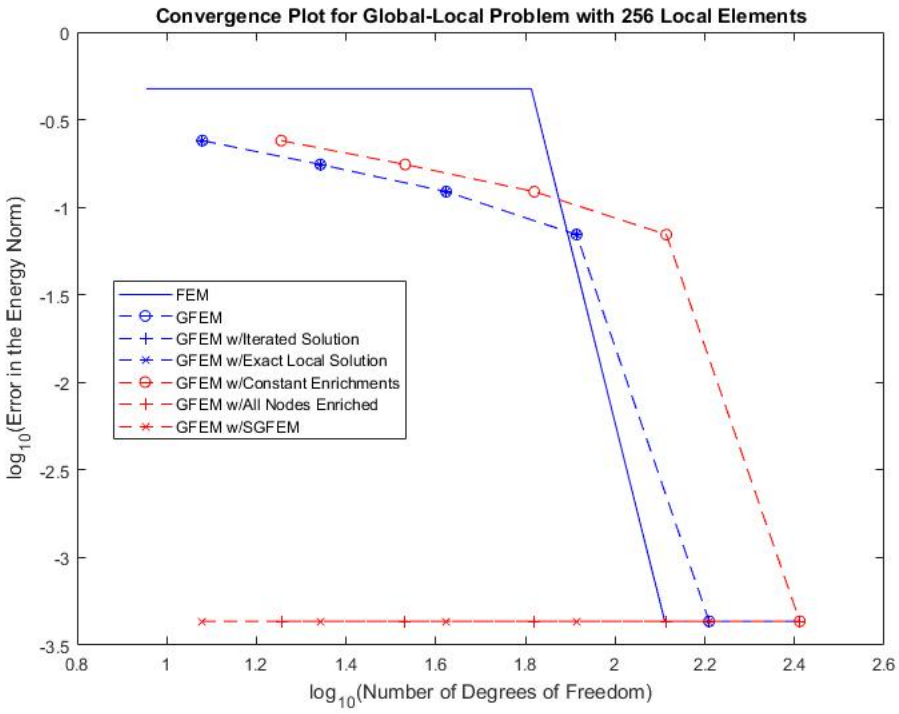


Figure 12: Convergence Plot with 256 Local Elements Used

Figure 12 above shows that the convergence plots for the GFEM solutions using iterated and exact local solutions show a similar result to the FEM convergence plot when 128 global elements(162 degrees of freedom) are used. There is an almost discontinuous jump in the error in the energy norm at this point despite showing linear convergence beforehand. The values of the error also match those shown in Figure 11 from 12 degrees of freedom to 82 degrees of freedom. The convergence plot for the GFEM using constant enrichments, like what was done in Figures 4 and 5, show similar results and convergence rates to the GFEM with and without iterated and exact local solutions. This is to be expected based on the similarities shown between Figures 2 to 5. The convergence plots for the GFEM solutions using SGFEM and fully enriching every node in the mesh show that there is no convergence and the error in the energy norm is close to zero and constant as the degree of freedoms increase. This is to be expected based on the results shown in Figures 6 to 9. The implication of these results will be discussed in the next

section.

# 5 Discussion

The results shown in Figures 2 and 3 demonstrate that the accuracy of the local solution compared to the exact solution does not impact the results of the GFEM solution. The GFEM solutions remain unchanged whether the local solution was accurate or not for all cases tested in Section 4. The results in Figures 2 to 9 demonstrates that the local solution need only capture the general behaviour of the heterogeneous material section to be able to approximate this in the GFEM solution. This is shown in Figures 2 to 5 as the GFEM solution is able to capture the localized features caused by the heterogeneous materials regardless of the local problem solutions accuracy. This behaviour can be attributed to the problem with blending elements existing in the GFEM mesh.

In blending elements, the partition of unity that is built in all other elements is lost since only a portion of the nodes in blending elements are enriched. This means that the enrichments in these elements cannot be exactly reproduced at all points which leads to errors in the blending elements and thus the rest of the solution. In Figures 2 to 5, the blending elements can be seen in the plots as the sections of the solutions that have "bubbles". This is because in the blending elements the GFEM shape functions are quadratic due to linear shape functions being used to approximate the local solution and linear shape functions being selected as the basis of functions to use in each global element. Thus, the resulting GFEM shape function is quadratic. This effect is seen in the blending elements and not the rest of the elements containing enrichments due to the loss of the partition of unity in these elements , thus the linear enrichment cannot be reproduced at each point and the quadratic term becomes the dominant approximation function in these elements. The errors that the blending elements produce can be seen in the previously mentioned plots as well. The solution approximates the exact solution up until the first blending element. After this point, the solution does not agree with the exact solution. It is worth noting that after the set of nodes enriched by the local solution, the approximate solution will correctly match the slope of the exact solution from the points $x$ equals 0.75 to one. However, the actual displacement values in this region will not be accurate

when compared to the exact solution.

To accurately approximate the model problem using GFEM and to obtain optimal convergence while using this method, the problem in the blending elements needed to be addressed. To do this, first a test case where every node in the GFEM mesh was enriched was explored to determine if the errors seen in Figures 2 to 5 were being caused by the blending elements. The results of this test case were shown in Figures 6 to 7 and these results showed that enriching every node stabilizes the GFEM stiffness matrix and convergence is achieved in only eight global elements. This result demonstrated that the errors previously seen were the result of parasitic terms arising in the stiffness matrices in the blending elements. Thus, SGFEM was applied to stabilize the conditioning of the stiffness matrix in the blending elements and reduce the resulting errors. Figures 8 to 9 show similar results to those obtained when all nodes were enriched, but with using less degrees of freedom since only the nodes in the set $I_h^e$ were enriched and SGFEM was only applied in the blending elements. This demonstrates that SGFEM can be applied to stabilize the conditioning of stiffness matrices produced in blending elements to reduce errors and obtain convergence in the GFEM approximation.

Stemming from these results, the various improvement methods discussed in Section 3.5 were applied to the model problem and compares it to using FEM exclusively. Figures 10 to 12 summarize the results obtained from applying each method at eight, 16, 32, 64, and 128 global elements with 64, 128, and 256 local elements respectively. From each figure, the results obtained using FEM to solve the model problem show a constant error in the energy norm until about 129 degrees of freedom (128 elements) are used, then there is an almost discontinuous jump in the accuracy of the strain energy. Using 128 elements or more cause the FEM solution to be significantly more accurate and the error will remain constant after this jump in accuracy as well. The FEM's approximation of the strain energy behaves this way because when using eight to 64 elements to approximate the solution the FEM mesh will capture an even number of white and black phases in each element within the heterogeneous material section ($\Omega = \{x|\frac{3L}{8} \leq x \leq \frac{5L}{8}\}$). This means that the FEM will approximate the material constant over these elements as an average of the material constants in each phase leading FEM to "see" a constant Young's modulus instead of a heterogeneous material. This leads the approximation to be constant until 128 elements are reached since each

phase is $\frac{L}{128}$ in length and thus at 128 elements a node is placed at each point where the material changes in the heterogeneous material section and FEM can accurately approximate the behavior of the solution.

This behavior with FEM shows why GFEM is appropriate to use here. The FEM method cannot accurately capture the behavior of the model problem without using a conforming mesh and placing a node at each point where a material change occurs. Figures 2 to 3 show that the GFEM can capture the general behavior of the heterogeneous materials with eight global elements. Figure 10 shows that the GFEM when compared to the FEM converges at a rate of 0.53 as the number of degrees of freedom increase. This demonstrates that using GFEM without any improvements to the local solution will slowly converge to the exact solution. However, this is far from the optimal convergence rate of two that would be desirable for this method which further demonstrates the errors the blending elements introduce into the solution. This plot also further cements that the accuracy of the local solution does not impact the GFEM approximation for a given number of global elements since the convergence plots for the GFEM approximations using the iterated and exact local solution match the results obtained from only using the first iteration local solution. Figure 11 shows that increasing the number of local elements used, again, does not impact the GFEM approximations and that the convergence rate remains linear and converges at the same value.

As mentioned, the blending element problem causes the global-local methods used fail to converge completely until a conforming GFEM mesh is used as shown in Figure 12. At 128 elements, the GFEM approximation agrees almost exactly with the exact strain energy as shown by the large jump in error in the energy norm. This jump occurs for the same reasons it occurred in the FEM, however, the GFEM enrichment functions allow the GFEM approximation to slowly converge since the ernichment can capture the localized behavior in the problem. The plot that shows the convergence plot for the GFEM approximation with constant enrichments used is identical to the GFEM approximation without any modifications, but shifted to the right due to a larger number of degrees of freedom used. This result agrees with what was observed in Figures 4 to 5 since the GFEM approximation was identical to that shown in Figures 2 to 3, but with every node being enriched instead of a subset of nodes. The main observation to note from Figure 12 is that the plots for using SGFEM and enriching every node with

the exact solution show complete convergence at eight global elements and then remains constant as the number of elements and degrees of freedom increase. This demonstrates further that the enrichment functions used were able to capture the localized behavior caused by the heterogeneous materials in the GFEM solution, but errors that were introduced into the solution by the blending elements prevented convergence from happening without using a conforming mesh. Once the blending elements were stabilized, via SGFEM or enriching every node, the GFEM solution converged completely.

# 6 Conclusion

This thesis presents a global-local approach through the framework of GFEM to solving problems with heterogeneities that impact the global response. Limitiations of using such approaches and various methods to improve the approximations obtained through using global-local methods with GFEM. The global-local method with GFEM was applied to a model problem that contains heterogeneous materials along with several improvements and modifications applied to the method to attempt to improve the approximations obtained. Of these methods, those applied included: iterating the local solution, using an exact local solution, applying SGFEM to blending elements, using constant enrichments, and enriching every node with the exact solution in a GFEM mesh. The accuracy and effectiveness of each method was analyzed using convergence plots to investigate the error in the strain energy and point-wise displacement plots.

The GFEM solutions were shown to be able to effectively capture the behaviour of the heterogeneous materials impact on the global solution. However, the GFEM with no modifications to the method was only able to capture the general impact of the heterogeneities and not the precise point-wise displacement values compared to the exact solution. Following this, the GFEM demonstrated that the local solutions accuracy imposed no change in the accuracy of the GFEM approximation. It was shown that if the local solution was able to capture the general behavior of the heterogeneities in the model problem, it would be reflected in the GFEM solution appropriately. The GFEM solution also demonstrated slight convergence as the number of global elements increased as well, until a conformin mesh was used to approximate the solution. Thus, this presented the need to modify the GFEM

process to obtain better convergence rates and more accurate approximations on coarser global meshes to reduce the number of degrees of freedom needed to solve the problem.

This led to the need to stabilize the blending elements to reduce errors and obtain convergence on coarser global meshes. SGFEM has been demonstrated to stabilize matrices with parasitic terms and improve convergence rates in a number of literature, thus it was applied to the same effect in the model problem explored. Applying SGFEM to the blending elements demonstrated the ability to reduce errors there and stabilize the stiffness matrices produced so that the GFEM solution can converge to the exact solution.

This thesis has shown that for problems that enrich a subset of nodes in a mesh and include heterogeneous materials, blending elements can cause errors to form in the solution due to the introduction of parasitic terms in their stiffness matrices. Stabilizing these elements through SGFEM or complete enrichment of nodes in a mesh fixes the conditioning of the stiffness matrices and reduces the effect of parasitic terms and reduce errors to allow the GFEM solution to converge to the exact solution on coarse mesh. This thesis has also shown, that for problems of similar to the model problem, the global-local techniques do not improve GFEM approximations with improved local solutions. The GFEM only requires the local solution capture the general behavior of localized features in a problem domain to be able to reflect these behaviors on a global-scale. Future work can include further investigation into applying a more accurate local solution as an enrichment to determine why the accuracy of the local problem does not impact the GFEM solution.

# References


1. Duarte, C. A., Simone, A., Aragon, A. M. (2018). Enriched Finite Element Methods: Theory and Practice.

2. Fries, T., Belytschko, T. (2010). The Extended/Generalized Finite Element Method: An Overview of the Method and its Application. International Journal for Numerical Methods in Engineering, 253-304.

3. Moës, N., Cloirec, M., Cartraud, P., Remacle, J. (2003). A compu-

tational approach to handle complex microstructure geometries. Computer Methods in Applied Mechanics and Engineering, 192(28-30), 3163-3177. doi:10.1016/s0045-7825(03)00346-3

4. Weinhardt, P. D., Debella, L. B., Arndt, M., Machado, R. D. (2018). Gfem Stabilization Techniques Applied To Dynamic Analysis Of Non-Uniform Section Bars. Latin American Journal of Solids and Structures, 15(11). doi:10.1590/1679-78254265

5. Mao, K. M., Sun, C. T. (1991). A refined global-local finite element analysis method. International Journal for Numerical Methods in Engineering, 32(1), 29-43. doi:10.1002/nme.1620320103

6. Plews, J., Duarte, C. (2014). Bridging multiple structural scales with a generalized finite element method. International Journal for Numerical Methods in Engineering, 102(3-4), 180-201. doi:10.1002/nme.4703

7. Szabo, B. A., Babuska, I. (2011). Introduction to finite element analysis: Formulation, verification, and validation. Hoboken, NJ: Wiley.

# Appendix: Solution Algorithm

GFEM matrices are inherently linealy depedent when polynomial enrichments are used, like in this thesis. The following iterative algorithm is used to solve the system of equations shown in Equation 26.

$$\tilde{K}\tilde{u} = \tilde{f} \tag{26}$$

Where $\tilde{K}$ is a positive semi-definitive(singular) matrix, $\tilde{u}$ is the solution vector and $\tilde{f}$ is the force vector. Define a matrix $K$, a vector $u$ and $f$ by Equations 27, 28, and 29 respectively below.

$$K = T\tilde{K}T \tag{27}$$
$$u = T^{-1}\tilde{u} \tag{28}$$
$$f = T\tilde{f} \tag{29}$$

Where $T$ is defined in Equation 30 below

$$T_{i,j} = \frac{\delta_{i,j}}{\sqrt{\tilde{K_{i,j}}}} \tag{30}$$

Where $\delta_(i,j)$ is the Kronecker delta and its values are equal to one when $i = j$ and zero everywhere else. Then Equation 26 can be rewritten with the above transformations as Equation 31 below.

$$Ku = f \tag{31}$$

The scaled matrix $K$ is then perturbed since its diagonal matrices are equal to one following the above transformations. The perturbed matrix $K_\epsilon$ is shown in Equation 32 below.

$$K_\epsilon = K + \epsilon I \tag{32}$$

Where $\epsilon$ is a small coefficient and $I$ is the identity matrix. The matrix $K_\epsilon$

is a positive definitive matrix and hence non-singular. The solution $u$ to the Equation 31 is then computed as follows. Let $u_0$ and $r_0$ be the initial solution to the system and the initial residual error in Equation 31. The calculations for $u_0$ and $r_0$ are shown in Equations 33 and 34 below.

$$u_0 = K_\epsilon^{-1} f \tag{33}$$
$$r_0 = f - K u_0 \tag{34}$$

Let the error be defined as $e_0 = u - u_0$, then $e_0$ can be calculated as Equation 35.

$$e_0 = K_\epsilon^{-1} r_0 \tag{35}$$

The iterative process is then given by Equations 36, 37, and 38 below.

$$r_i = r_0 - \sum_{j=0}^{i-1} K e_j \tag{36}$$
$$e_i = K_\epsilon^{-1} r_i \tag{37}$$
$$u_i = u_0 + \sum_{j=0}^{i-1} e_j \tag{38}$$

This process is repeated for $i \geq 1$ until the value defined by $|\frac{e_i K e_i}{u_i K u_i}|$ is sufficiently small. The solution to the system shown in Equation 26 is then given by Equation 39 below.

$$\tilde{u} = Tu \tag{39}$$